Training-Free Generation of Diverse and High-Fidelity Images via Prompt Semantic Space Optimization

Debin Meng¹ Chen Jin² Zheng Gao¹ Yanran Li³ Ioannis Patras¹ Georgios Tzimiropoulos^{1,4}

¹Queen Mary University of London, ²Centre for AI, AstraZeneca, UK, ³University of Bedfordshire, ⁴Samsung AI Center, UK

{debin.meng, z.gao, i.patras, g.tzimiropoulos}@qmul.ac.uk, chen.jin@astrazeneca.com

Yanran.Li@beds.ac.uk

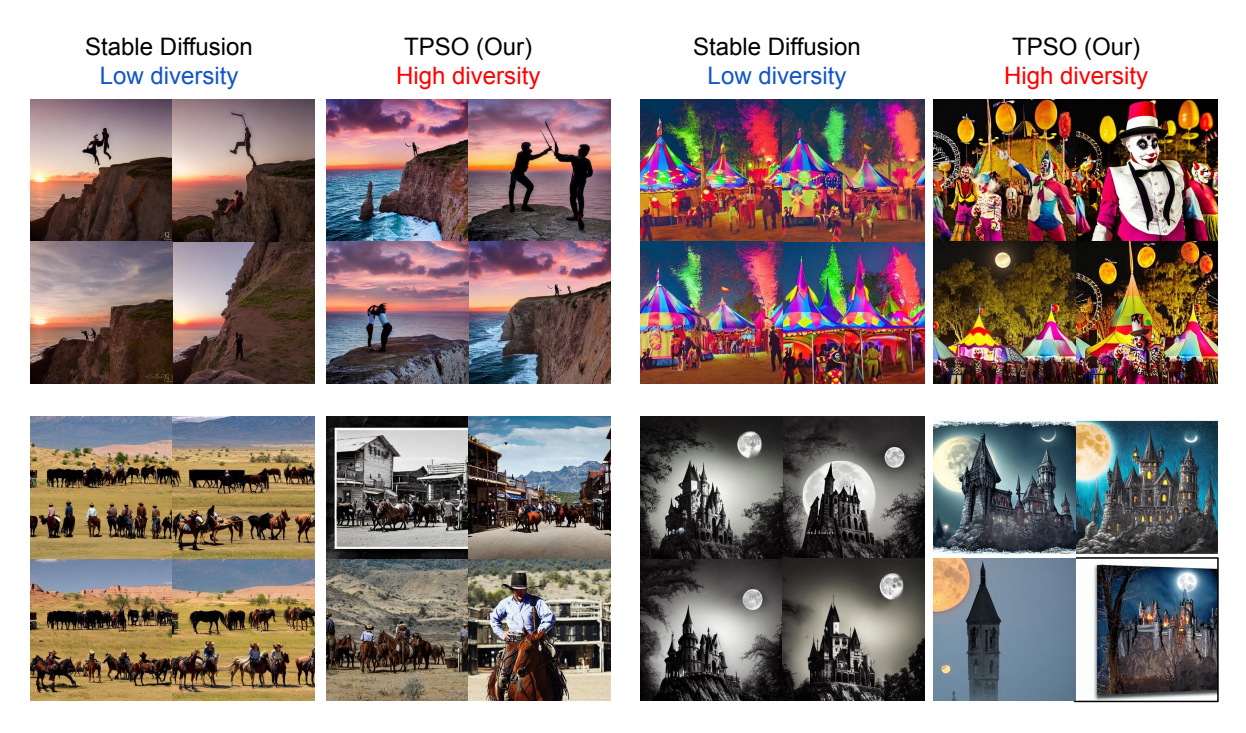


Figure 1. Baseline diffusion models tend to produce low-diversity or nearly repeated outputs across sampling runs, leading to redundant sampling efforts. In contrast, our approach enhances output diversity, yielding a broader range of plausible and distinct visual outcomes.

Abstract

Image diversity remains a fundamental challenge for text-to-image diffusion models. Low-diversity models tend to generate repetitive outputs, increasing sampling redundancy and hindering both creative exploration and downstream applications. A primary cause is that generation often collapses toward a strong mode in the learned distribution. Existing attempts to improve diversity, such as noise resampling, prompt rewriting, or steering-based guidance—often still collapse to dominant modes or introduce distortions that degrade image quality. In light of this, we propose Token—Prompt embedding Space Optimization (TPSO), a training-free and model-agnostic module.

TPSO introduces learnable parameters to explore underrepresented regions of the token embedding space, reducing the tendency of the model to repeatedly generate samples from strong modes of the learned distribution. At the same time, the prompt-level space provides a global semantic constraint that regulates distribution shifts, preventing quality degradation while maintaining high fidelity. Extensive experiments on MS-COCO and three diffusion backbones show that TPSO significantly enhances generative diversity—improving baseline performance from 1.10 to 4.18 points—without sacrificing image quality. Code will be released upon acceptance.

1. Introduction

Powered by recent developments in diffusion models [9, 24] and contrastively trained text encoders [18], modern textto-image systems are now capable of producing visually compelling and semantically faithful images from diverse natural-language prompts [20]. A fundamental attribute of generative models is their ability to produce diverse outputs under the same condition. Ideally, a generative model should generate samples that are both consistent with the conditioning input and diverse in appearance. For example, a prompt describing "a wooden chair" can yield many valid outcomes that differ in shape, material texture, or stylistic design. However, current diffusion models often suffer from limited diversity, resulting in repetitive generations. This lack of diversity not only leads to redundant resampling and increased computational cost but also constrains creative exploration and impairs downstream applications such as data generation for model training-where repetitive samples can cause overfitting and reduce dataset utility. Although recent diffusion models have achieved stronger conditional alignment and higher image fidelity, they exhibit an increasing tendency toward reduced diversity [1]. This phenomenon stems largely from mode collapse, where a substantial portion of generated samples converge toward strong modes within the learned distribution, leading to repetitive and less diverse outcomes.

To enhance diversity in image generation, a naive approach is to resample the initial noise. However, this strategy cannot effectively control the degree of diversity and often leads to visually similar outputs [2]. Another straightforward solution is to automatically modify input prompts using large language models (LLMs) such as ChatGPT. Yet, these methods rely on external models, introducing substantial computational overhead, and introduce lengthy promptgeneration procedures. Moreover, both noise resampling and prompt modification ultimately still draw samples from the dominant modes of the learned distribution, and thus fail to produce genuinely diverse images. Another line of research seeks to improve diversity by optimizing intermediate latents [3] or manipulating text embeddings [21] to enforce separation between samples. While these approaches can produce diverse outputs, they often suffer from instability: promoting diversity in this manner frequently introduces unintended distortions into the generated images, leading to degradation in overall image quality.

To address these limitations, we introduce Token–Prompt Space Optimization (TPSO), a simple yet effective optimization strategy that directly tackles the two root causes of low diversity, generation from strong mode of distribution and distortion-induced quality decay. The core idea of TPSO is to jointly operate in two complementary representation spaces. First, TPSO steers learnable parameters to explore the underutilized token embedding space, enabling the model to escape strong modes of the learned distribution and generate more diverse variants. Second, TPSO constrains this exploration within the prompt embedding space, using semantic alignment losses to prevent distribution shifts and avoid the distortions commonly observed in prior methods. This ensures that the generated variants remain faithful to the original prompt while maximizing inter-sample diversity.

Importantly, TPSO achieves these effects without introducing any external models, or additional training. It reuses the CLIP encoder already embedded in modern diffusion systems, making it fully training-free, lightweight, and model-agnostic. As a result, TPSO integrates seamlessly into existing text-to-image pipelines and enhances generative diversity without compromising fidelity.

Our key contributions are summarized as follows:

- We propose a generic, lightweight, training-free and model-agnostic strategy that enhances generative diversity in existing diffusion pipelines without modifying model architectures or adding new modules.
- We propose a dual-space optimization objective, TPSO jointly explores the token embedding space to escape strong-mode collapse and leverages the prompt embedding space as a semantic constraint to prevent distribution shift, achieving a robust balance between diversity and fidelity.
- Extensive experiments on MS-COCO and three diffusion backbones show that TPSO substantially improves sample diversity (outperforming prior approaches from 1.10 to 4.18) while maintaining image quality and text-image alignment,

2. Related work

Conditional image generation has attracted substantial attention from both academia and industry due to its ability to synthesize realistic and aesthetically compelling images. This technology underpins a wide range of applications in design, entertainment, advertising, and creative content generation. To improve controllability and alignment with user intent, conditional generative models guide the generation process through explicit input signals such as text [20], reference images [10, 16, 22], or spatial layouts [12, 27]. Recent works further explore multi-modal conditioning—such as combining text and layout [17, 26] to increase semantic control and fidelity. Despite these advances, most existing efforts primarily focus on improving image quality and conditional alignment, while overlooking another fundamental attribute of generative models—diversity. The ability to produce multiple valid outputs under the same condition is essential for creative exploration and for supporting robust downstream applications, yet remains insufficiently explored in current diffusionbased methods [1].

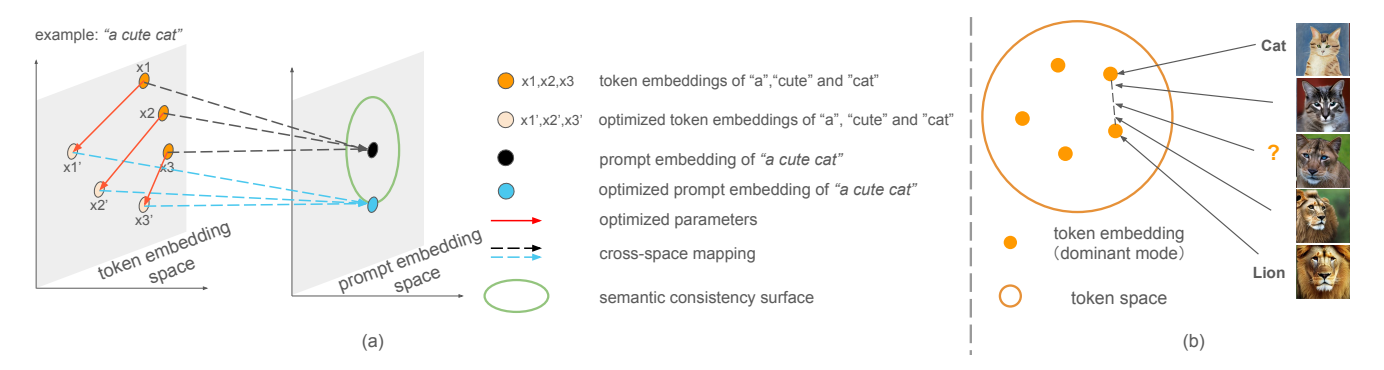


Figure 2. Overview of how our method explores underrepresented regions in the token embedding space under semantic constraints while avoiding explores invalid regions that cause semantic drift. (a) TPSO updates token embeddings away from the default fixed embeddings (orange) toward underrepresented regions. The green semantic-consistency surface conceptually represents our semantic constraint, ensuring that the resulting prompt embeddings remain meaning-preserving. (b) Interpolating between the token embeddings for 'cat' and 'lion' produces smooth semantic transitions, revealing underrepresented yet meaningful regions. However, drifting too far leads to invalid exploration, where semantic alignment breaks and generated images begin to swap or mix characteristics of 'cat' and 'lion'.

Diversity Image generation Diversity reflects a generative model's ability to produce varied outputs from the same input condition—for example, generating different images of "a dog" from a single prompt. Models with low diversity tend to produce repetitive outputs, covering only a narrow region of the learned distribution. Classical diffusion models such as DDPM [9] inherently support diverse sampling, which contains randomness at each denoising step. However, DDPM requires hundreds to thousands of inference steps, limiting its practicality in real-world applications. DDIM [24] addresses this by reducing the number of steps while maintaining generation quality, enabling faster sampling with preserved diversity. Recent studies have highlighted that modern diffusion models increasingly prioritize image fidelity and prompt alignment, often at the expense of their ability to generate diverse outputs [1]. A common strategy for inducing diversity is to resample the initial noise or repeatedly run the diffusion process; however, such approaches offer little control over the diversity level and typically re-converge to similar visual modes [2]. Another direction modifies prompts through large language models (LLMs), but this introduces substantial external computation and still tends to sample from dominant regions of the learned distribution. Beyond these heuristic methods, prior works attempt to impose diversity by perturbing intermediate latents [3] or adjusting text embeddings [21]. While effective in separating samples, these techniques often drive the generation trajectory into unstable regions of the latent space, resulting in artifacts or semantic drift. A concurrent approach [25] trains a prompt encoder to generate multiple alternative prompts for increased diversity. However, this strategy requires additional training and does not explicitly address escaping strong mode of the model's learned distribution. In contrast, our method is entirely trainingfree and operates by directly exploring underutilized tokenembedding subspaces, while applying semantic constraints in the prompt-embedding space to preserve fidelity. This design makes TPSO lightweight, model-agnostic, and readily applicable to a wide range of diffusion backbones without retraining.

3. Preliminary

3.1. CLIP Text Encoder

CLIP text encoder [18] is a standard component in modern text-to-image generation systems, including Stable Diffusion [20, 23] and DALL·E [19]. Given a prompt c with tokens $\{i_1,\ldots,i_N\}$, the encoder first maps each token to its embedding through a deterministic matrix indexing $\mathbf{e}_n = M[i_n]$, where $M \in \mathbb{R}^{V \times d}$ is the embedding matrix. We refer to this module as the *token encoder*. The resulting token embeddings are then contextualized by a Transformer-based *prompt encoder*, producing $y = E(\mathbf{e}_1,\ldots,\mathbf{e}_N)$, which serves as textual conditioning for the diffusion model. In original clip, a lightweight *prompt projector* further maps these contextualized features into the image-text aligned space, ensuring alignment between the text encoder and the image encoder of clip.

3.2. Classifier-Free Guidance (CFG)

Classifier-Free Guidance (CFG) [8] is a standard practice in current diffusion models and is regarded as a key factor enabling conditional alignment and high-quality image synthesis. It interpolates conditional and unconditional denoising predictions:

$$\hat{\epsilon}_{\theta}(x_t, c) = \epsilon_{\theta}(x_t, \emptyset) + \omega \Big(\underbrace{\epsilon_{\theta}(x_t, c) - \epsilon_{\theta}(x_t, \emptyset)}_{\text{guidance direction}}\Big), \quad (1)$$

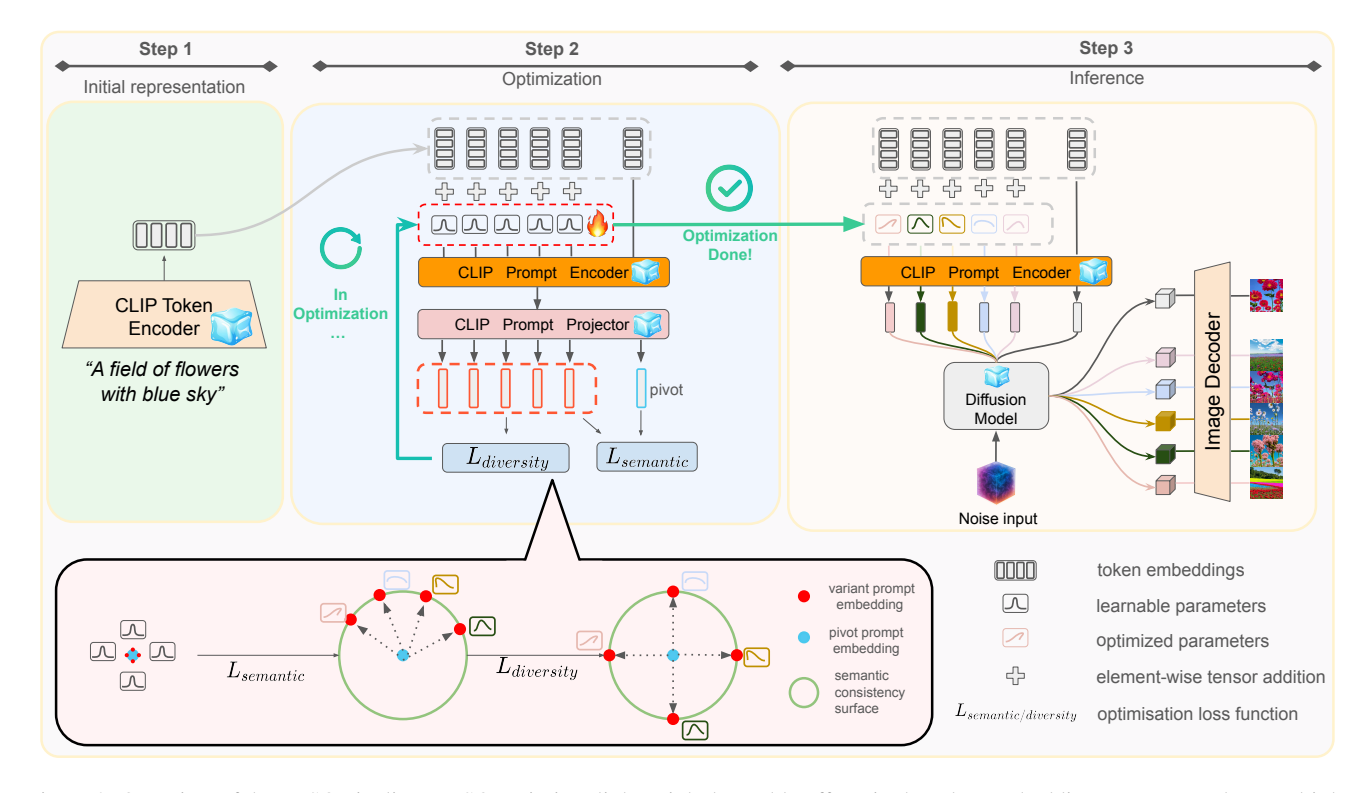


Figure 3. Overview of the TPSO pipeline. TPSO optimizes lightweight learnable offsets in the token embedding space to produce multiple semantically aligned prompt variants, which induce diverse conditional representations and yield different CFG guidance directions. This enables substantially richer generative diversity, all without modifying the diffusion model or introducing any additional components.

where ω controls guidance strength. The vector $d_c = \epsilon_{\theta}(x_t,c) - \epsilon_{\theta}(x_t,\emptyset)$ represents the semantic guidance direction. While CFG substantially boosts faithfulness to the conditioning signal, it also induces a critical side effect: reduced diversity [8]. Under strong guidance, generated samples tend to collapse toward a narrow semantic modes, failing to reflect the range of diverse appearances that the same prompt could correspond to.

Escaping the strong mode of the learned distribution.

Mode collapse arises because the CFG direction is determined by the output of the prompt encoder, which typically lies in a *strong mode* of its learned prompt distribution. As a result, its overall semantic tendency consistently steers the diffusion trajectory toward a narrow, high-density region of latent space, thereby limiting generative variability.

To address this, we diversify the *source* of the guidance direction. Instead of relying on a single prompt embedding anchored in the strong mode, we optimize multiple *variant prompt embeddings* within the token–prompt space. Each variant provides a distinct conditional representation $c^{(k)}$ drawn from underrepresented regions of the embedding space, thereby inducing a different CFG direction $d_c^{(k)}$:

$$d_c^{(k)} = \epsilon_\theta(x_t^{(k)}, c^{(k)}) - \epsilon_\theta(x_t^{(k)}, \emptyset). \tag{2}$$

These variant directions steer the diffusion process along alternative latent trajectories $\boldsymbol{x}_t^{(k)}$, enabling exploration beyond the strong mode at each timestep. This mechanism forms the core of our approach to achieving higher diversity without compromising semantic fidelity.

4. Method

Textual Inversion [6] reveals that exploring the token space of a pre-trained text encoder in Stable Diffusion can encode novel visual concepts beyond the original training domain. This observation suggests that the token embedding space contains underutilized semantic regions, motivating our approach to leverage this latent capacity to escape strong modes of learned distribution and promote diverse generation.

However, directly exploring the token space is challenging in practice. Different prompts contain varying numbers of tokens, and each token contributes unevenly and often unpredictably to the final output. To semantically explore meaningful token regions, we further utilize the global prompt embedding space. We apply a diversity loss in this space to encourage exploration toward maximally diverse

Algorithm 1 Optimization of Learnable Token Offsets

- 1: **Input:** Token embeddings e_{token} , learnable offsets ε
- 2: **Output:** Optimized learnable offsets ε
- 3: Initialize $\varepsilon \sim \mathcal{N}(0, 10^{-4})$
- 4: Compute $\mathbf{v} = f(E(e_{\text{token}}))$
- 5: Compute $\mathbf{v}' = f(E(e_{\text{token}} + \varepsilon))$ (Eq. 5 and 6)
- 6: repeat
- 7: Update $\varepsilon \leftarrow \operatorname{Adam}(\varepsilon, \nabla_{\varepsilon} \mathcal{L}_{\text{ioint}})$ (Eq. 9)
- 8: Recompute $\mathbf{v}' = f(E(e_{token} + \boldsymbol{\varepsilon}))$
- 9: **until** $\mathcal{L}_{\text{semantic}}$ convergence
- 10: **return** ε

pairwise generations. In addition, we introduce a semantic alignment loss that maintains alignment with the original prompt while preventing distribution shifts that could lead to quality degradation. We provide a detailed description of the token and prompt spaces in Section 4.1, followed by the formulation of semantic regularization in Section 4.2 and the diversity objective in Section 4.3.

4.1. Variant Token and Prompt Embedding

As illustrated in Figure 3, our method operates on the text encoder of Stable Diffusion. Let $\{i_1, \ldots, i_n\}$ denote the input prompt tokens, and let

$$e_{\text{token}} = \{\mathbf{e}_1, \dots, \mathbf{e}_n\}, \qquad \mathbf{e}_i \in \mathbb{R}^d,$$
 (3)

be their corresponding fixed CLIP token embeddings obtained via deterministic matrix indexing $\mathbf{e}_n = M[i_n]$, where $M \in \mathbb{R}^{V \times d}$ (Section 3.1).

To enable controllable variation, we introduce a set of learnable token-level offset parameters

$$\boldsymbol{\varepsilon} = \{\varepsilon_1, \dots, \varepsilon_n\}, \qquad \varepsilon_i \in \mathbb{R}^d.$$
 (4)

and define the resulting variant token embeddings as

$$e_{\text{token}} + \varepsilon = \{\mathbf{e}_1 + \varepsilon_1, \ \mathbf{e}_2 + \varepsilon_2, \ \dots, \ \mathbf{e}_n + \varepsilon_n\}.$$
 (5)

These variant embeddings are then passed through the CLIP prompt encoder E and projector network f to obtain prompt-level embeddings:

$$\mathbf{v} = f(E(e_{\text{token}})), \quad \mathbf{v}' = f(E(e_{\text{token}} + \varepsilon)), \quad (6)$$

where both $\mathbf{v}, \mathbf{v}' \in \mathbb{R}^d$ represent the original and offset-induced prompt embeddings, respectively. These embeddings constitute the basis for the semantic alignment and diversity objectives introduced in Section 4.2 and Section 4.3.

4.2. Semantic Optimization Target

We optimize the learnable offset parameters ε such that the resulting variant embeddings remain within a semantically valid region of the prompt space. This constraint ensures

that the generated variants preserve the semantic meaning of the original prompt while avoiding distribution shifts that may degrade perceptual quality.

To enforce this, we define a semantic alignment loss. Since the CLIP prompt embedding space is explicitly structured according to cosine similarity (e.g. CLIP Score [18]), we measure semantic deviation using the cosine similarity between the original prompt embedding ${\bf v}$ and each offset-induced embedding ${\bf v}'_i$. We optimization objective (Algorithm 1) requires each similarity value to fall within a tolerance band centered at a target threshold κ (e.g., 0.80), with $\sigma=0.01$ controlling the allowable deviation:

$$\mathcal{L}_{\text{semantic}} = \sum_{i=1}^{N} \max(0, |\cos(\mathbf{v}, \mathbf{v}_i') - \kappa| - \sigma).$$
 (7)

We use a summation rather than an average over N variants because each variant is governed by its own independent set of learnable offsets, and thus their gradients should not be normalized across variants.

4.3. Diversity Optimization Target

To encourage the generated image variants to be diverse rather than redundant, we introduce a diversity loss applied to the set of variant prompt embeddings $\mathbf{v}' = \{\mathbf{v}_1', \dots, \mathbf{v}_N'\}$. This loss penalizes high similarity between any pair of variants:

$$\mathcal{L}_{\text{div}} = \frac{1}{N(N-1)} \sum_{i=1}^{N} \sum_{\substack{j=1\\j\neq i}}^{N} \cos(\mathbf{v}_i', \mathbf{v}_j'). \tag{8}$$

The overall objective combines semantic preservation and diversity enhancement:

$$\mathcal{L}_{\text{joint}} = \mathcal{L}_{\text{semantic}} + \lambda \cdot \mathcal{L}_{\text{div}}, \tag{9}$$

where λ controls the strength of the diversity term. The full optimization procedure is provided in Algorithm 1.

Progressive Embedding Scheduler. Although the optimized variant embeddings improve diversity, using them throughout the entire sampling trajectory may introduce mild distribution shifts in the late denoising stages, where Stable Diffusion refines fine-grained details. To balance diversity and fidelity, we employ a simple ratio-based scheduler. Diffusion sampling proceeds from timestep T (e.g., 1000) down to 1. Given a proportion parameter $r \in [0,1]$, the early timesteps (from t=T down to T(1-r)) use the optimized embedding with a progressive interpolation back to the original embedding, while the remaining timesteps use the original embedding only. Let y and y' denote the original and the optimized embedding respectively:

Table 1. Main comparison results on 50k samples. Our primary evaluation focuses on diversity (Recall, MSS, Vendi) and the main quality metric (FID), highlighted in **dark**. The slight decrease in CLIP Score is expected and remains trivial relative to the diversity improvements. Precision also shows minor reductions. However, this should not be interpreted as quality degradation, as Precision can penalize high-quality yet diverse samples simply because they fall outside the reference-image manifold.

	Quality		Consistency	Diversity		
Method	FID ↓	Precision ↑	CLIP↑	Recall ↑	MSS ↓	Vendi ↑
Stable Diffusion 1.5	20.093	0.610	31.700	0.542	0.231	5.558
Dynamic CFG	20.405	0.606	31.170	0.477	0.359	2.560
CADS	19.750	0.602	30.940	0.544	0.198	5.933
Particle Guidance	19.990	0.572	31.320	0.569	0.194	6.387
TPSO	18.191 (-1.902)	0.608 (-0.002)	31.100 (-0.6)	0.618 (+0.076)	0.158 (-0.073)	6.705 (+1.147)
Stable Diffusion 2.1	19.871	0.599	31.880	0.557	0.247	5.237
Dynamic CFG	24.823	0.601	30.960	0.413	0.355	2.608
CADS	19.891	0.599	31.370	0.536	0.221	5.524
Particle Guidance	19.757	0.595	31.840	0.541	0.243	5.298
TPSO	17.569 (-2.302)	0.571 (-0.028)	31.100 (-0.780)	0.647 (+0.090)	0.137 (-0.110)	7.299 (+2.062)
Stable Diffusion 3.5	24.567	0.645	32.070	0.442	0.369	2.828
Dynamic CFG	23.943	0.574	31.310	0.420	0.350	2.739
CADS	26.934	0.639	31.760	0.446	0.277	4.359
Particle Guidance	24.275	0.638	32.190	0.498	0.385	2.562
TPSO	23.623 (-0.944)	0.576 (-0.069)	31.930 (-0.140)	0.546 (+0.104)	0.156 (-0.213)	7.010 (+4.182)

$$y_t^* = \alpha_t y' + (1 - \alpha_t) y, \tag{10}$$

where

$$\alpha_t = \begin{cases} 0, & t \le T(1-r), \\ \frac{t - T(1-r)}{rT}, & T(1-r) < t \le T. \end{cases}$$
 (11)

This design takes advantage of the coarse-to-fine nature of diffusion sampling: early steps determine the global structure and benefit most from the optimized embeddings to promote diverse generation, whereas later steps refine texture and appearance, which are best guided by the original embedding to preserve visual quality. We find that setting $r \in [0.3, 0.5]$ provides high diversity while preserving image quality.

5. Experiments

5.1. Experimental Settings

Implementation Details. To verify that TPSO is model-agnostic, we evaluate it across three representative text-to-image generators: (1) Stable Diffusion 1.5 (SD1.5) and Stable Diffusion 2.1 (SD2.1), both based on the denoising diffusion framework [9, 20, 24]. And (2) Stable Diffusion 3.5 (SD3.5) [4], which adopts a rectified-flow formulation [14, 15]. We follow their default public configurations. Details can be found in the supplementary materials.

All experiments use fixed random seeds to ensure fair and model-consistent comparisons.

Dataset. We conduct experiments on the MSCOCO validation set [13]. Following standard evaluation protocols, we randomly sample 5,000 captions and generate 10 images per caption, resulting in 50k generated samples for each model–method pair. For ablation studies, we use a smaller subset of 1,000 captions (10k samples), consistent with the protocol in CADS [21].

5.2. Evaluation Metrics

Our goal is to enhance *diversity* without compromising *image quality* or *text-image alignment*. Therefore, we evaluate our method across three complementary aspects: **quality**, **conditional alignment**, and **diversity**.

Diversity Metrics. We report Recall [11] to quantify the coverage of the real data distribution, reflecting global diversity. For per-prompt (intra-set) diversity, we use the Mean Similarity Score (MSS) and Vendi Score [5], both computed using SSCD features following [21]. Lower MSS and higher Vendi indicate greater within-prompt variation.

Quality Metrics. We evaluate visual fidelity using Fréchet Inception Distance (FID) [7], which serves as our primary quality metric. We additionally report Precision [11], which offers a complementary perspective on fidelity. However, we find that Precision can wrongly penalize high quality, diverse samples simply because they fall outside the reference-image manifold, even though they remain visually plausible and semantically aligned (see supplementary



Figure 4. TPSO produces a wide range of visually distinct yet semantically faithful variants, demonstrating its ability to increase diversity without sacrificing image quality. In contrast, baseline diffusion models generate highly repetitive outputs across different sampling runs, revealing limited diversity and a strong tendency to remain near dominant patterns in the learned distribution.

material).

Alignment Metric. Text-image consistency is evaluated using the CLIP Score [18], defined as the cosine similarity between CLIP embeddings of the generated image and its corresponding prompt.

5.3. Qualitative Results.

Our objective is to increase image diversity while preserving visual fidelity and maintaining alignment with the input text. This target is challenging, as diversity gains should not introduce artifacts or semantic drift. As shown in Figure 4, baseline methods tend to produce visually similar results—often repeating similar layouts or structures even when different noise seeds are used. This highlighting the limited diversity of current diffusion models. In contrast, our method produces a broader range of plausible variations, exhibiting differences in geometry color, and finegrained details while remaining faithful to the prompt.

Importantly, TPSO achieves this diversity without degrading image quality. Unlike Dynamic CFG and CADS, which often improve diversity at the expense of weakened text alignment or visual quality.

5.4. Quantitative Results

Table 1 summarizes the quantitative performance across all baselines and diffusion backbones. TPSO consistently im-

Table 2. Impact of Semantic Retention Degree κ

κ	FID ↓	Precision ↑	CLIP ↑	Recall ↑	MSS ↓	Vendi ↑
0.70	49.686	0.591	30.610	0.578	0.122	7.559
0.75	49.799	0.610	30.930	0.549	0.142	7.099
0.80	49.575	0.598	31.140	0.514	0.161	6.646
0.85	50.377	0.597	31.330	0.475	0.177	6.388
0.90	52.298	0.617	31.560	0.357	0.226	5.201

proves all diversity metrics (Recall, MSS, and Vendi) while also achieving better FID, our primary quality indicator. This demonstrates that TPSO effectively enhances diversity without sacrificing overall image fidelity.

Although Precision shows a slight decrease, our experiments reveal that this drop stems from the limitation of Precision itself when evaluating diversity- oriented generation methods. As discussed in section C.3 of the supplementary material, Precision tends to reject high-quality but creativity samples, explains the observed decline and should not be interpreted as a loss of fidelity.

As expected, TPSO exhibits minor reductions in CLIP Score. As our method introduces learnable offsets in the prompt embedding space, which may cause small—but controlled—semantic shifts. However, these changes are marginal (less than 0.78 absolute difference) and negligible compared to the substantial gains in diversity and FID.

w/o diversity loss

w/ diversity loss more diversity



Figure 5. Across three diffusion backbones (from top to bottom: SD1.5, SD2.1, and SD3.5), incorporating the diversity loss produces a broader range of plausible variations with richer structural and fine-grained differences, while maintaining visual fidelity. Each group compares generations with and without the diversity loss under the same prompt and sampling setup.

Table 3. Impact of the proportion of steps r that apply optimized embedding variants.

r	FID↓	Precision ↑	CLIP ↑	Recall ↑	MSS ↓	Vendi ↑
0.2	52.042	0.626	31.45	0.432	0.217	5.249
0.4	49.575	0.598	31.14	0.514	0.161	6.646
0.6	50.063	0.617	30.96	0.548	0.146	7.051
-0.4	63.527	0.621	31.63	0.115	0.493	1.098

5.5. Ablation study

Semantic Retention Degree κ controls how closely each variant prompt embedding remains aligned with the original prompt in the prompt-embedding space. A higher κ enforces stronger semantic preservation, whereas a lower κ allows larger deviations introduced by the learnable offset parameters. As shown in Table 2, decreasing κ increases the allowable token space deviation, which leads to lower CLIP Scores but higher diversity. In practice, we find that

Table 4. Impact of the diversity-loss weight λ .

λ	FID ↓	Precision ↑	CLIP↑	Recall ↑	MSS ↓	Vendi ↑
0.0	49.575	0.598	31.140	0.514	0.161	6.646
2.5	49.672	0.624	31.130	0.537	0.149	6.894
5.0	49.376	0.619	31.040	0.539	0.138	7.134
7.5	48.860	0.618	30.940	0.537	0.127	7.380
10	48.543	0.618	30.890	0.568	0.121	7.539

setting $\kappa=0.80$ yields consistently strong diversity while preserving high semantic fidelity.

Effect of Diversity Loss and Weight λ . As shown in Table 4, larger diversity-loss weights λ induce stronger intra-prompt variation, leading to more diverse generations. However, the resulting larger learnable offsets also cause a gradual decline in CLIP score.

Effect of the ratio r. The ratio r determines how much the optimized embeddings are injected during sampling. Positive values (e.g., r=0.4) apply the optimized embeddings only in the first 40% of the coarse denoising steps to maximize diversity, and then gradually revert to the original embedding to preserve fidelity. Negative values (e.g., r=-0.4) invert this schedule, applying the optimized embeddings only in the final refinement stages, serving as a control to test the necessity of the coarse-to-fine design.

As shown in Table 3, early-stage variation (r>0) yields substantially higher diversity while maintaining visual fidelity, whereas late-stage variation (r<0) offers minimal diversity gains and noticeably degrades quality. These results validate our motivation: injecting variation during coarse steps enables diverse global structures, while restoring the original embedding during later refinement protects overall image quality.

6. Conclusion

We presented TPSO, a training-free and model-agnostic module for enhancing diversity in text-to-image generation without sacrificing visual fidelity or text-image alignment. By jointly optimizing learnable offsets in the token space and regulating their semantic deviation through the prompt-space representation, TPSO enables controlled exploration of underutilized semantic directions while maintaining consistency with the original prompt. Our dualspace objective effectively balances diversity and fidelity, allowing the diffusion process to escape dominant modes without introducing semantic drift. Extensive experiments across SD1.5, SD2.1, and SD3.5 demonstrate that TPSO consistently improves per-prompt and global diversity metrics while preserving image quality and conditional alignment, outperforming existing baselines such as Dynamic CFG, CADS and Particle Guidance. Given its simplicity, generality, and compatibility with modern diffusion and rectified-flow models, TPSO offers a practical and widely applicable approach for diversity-enhanced image generation.

References

- [1] Pietro Astolfi, Marlene Careil, Melissa Hall, Oscar Mañas, Matthew Muckley, Jakob Verbeek, Adriana Romero Soriano, and Michal Drozdzal. Consistency-diversity-realism pareto fronts of conditional image generative models. arXiv preprint arXiv:2406.10429, 2024. 2, 3
- [2] Yuanhao Ban, Ruochen Wang, Tianyi Zhou, Boqing Gong, Cho-Jui Hsieh, and Minhao Cheng. The crystal ball hypothesis in diffusion models: Anticipating object positions from initial noise. arXiv preprint arXiv:2406.01970, 2024. 2, 3
- [3] Gabriele Corso, Yilun Xu, Valentin De Bortoli, Regina Barzilay, and Tommi Jaakkola. Particle guidance: non-iid diverse sampling with diffusion models. *arXiv preprint arXiv:2310.13102*, 2023. 2, 3
- [4] Patrick Esser, Sumith Kulal, Andreas Blattmann, Rahim Entezari, Jonas Müller, Harry Saini, Yam Levi, Dominik Lorenz, Axel Sauer, Frederic Boesel, et al. Scaling rectified flow transformers for high-resolution image synthesis. In Forty-first international conference on machine learning, 2024. 6
- [5] Dan Friedman and Adji Bousso Dieng. The vendi score: A diversity evaluation metric for machine learning. arXiv preprint arXiv:2210.02410, 2022. 6
- [6] Rinon Gal, Yuval Alaluf, Yuval Atzmon, Or Patashnik, Amit H. Bermano, Gal Chechik, and Daniel Cohen-Or. An image is worth one word: Personalizing text-to-image generation using textual inversion, 2022. 4
- [7] Martin Heusel, Hubert Ramsauer, Thomas Unterthiner, Bernhard Nessler, and Sepp Hochreiter. Gans trained by a two time-scale update rule converge to a local nash equilibrium. In Neural Information Processing Systems, 2017. 6
- [8] Jonathan Ho and Tim Salimans. Classifier-free diffusion guidance. arXiv preprint arXiv:2207.12598, 2022. 3, 4
- [9] Jonathan Ho, Ajay Jain, and Pieter Abbeel. Denoising diffusion probabilistic models. Advances in neural information processing systems, 33:6840–6851, 2020. 2, 3, 6
- [10] Jonathan Ho, Chitwan Saharia, William Chan, David J Fleet, Mohammad Norouzi, and Tim Salimans. Cascaded diffusion models for high fidelity image generation. *Journal of Machine Learning Research*, 23(47):1–33, 2022. 2
- [11] Tuomas Kynkäänniemi, Tero Karras, Samuli Laine, Jaakko Lehtinen, and Timo Aila. Improved precision and recall metric for assessing generative models. Advances in neural information processing systems, 32, 2019. 6
- [12] Cheng-Han Lee, Ziwei Liu, Lingyun Wu, and Ping Luo. Maskgan: Towards diverse and interactive facial image manipulation. In *IEEE Conference on Computer Vision and Pattern Recognition (CVPR)*, 2020.
- [13] Tsung-Yi Lin, Michael Maire, Serge Belongie, James Hays, Pietro Perona, Deva Ramanan, Piotr Dollár, and C Lawrence Zitnick. Microsoft coco: Common objects in context. In Computer vision–ECCV 2014: 13th European conference, zurich, Switzerland, September 6-12, 2014, proceedings, part v 13, pages 740–755. Springer, 2014. 6
- [14] Yaron Lipman, Ricky TQ Chen, Heli Ben-Hamu, Maximilian Nickel, and Matt Le. Flow matching for generative modeling. arXiv preprint arXiv:2210.02747, 2022. 6

- [15] Xingchao Liu, Chengyue Gong, and Qiang Liu. Flow straight and fast: Learning to generate and transfer data with rectified flow. arXiv preprint arXiv:2209.03003, 2022. 6
- [16] Andreas Lugmayr, Martin Danelljan, Andres Romero, Fisher Yu, Radu Timofte, and Luc Van Gool. Repaint: Inpainting using denoising diffusion probabilistic models. In *Proceedings of the IEEE/CVF conference on computer vision and pattern recognition*, pages 11461–11471, 2022. 2
- [17] Debin Meng, Christos Tzelepis, Ioannis Patras, and Georgios Tzimiropoulos. Mm2latent: Text-to-facial image generation and editing in gans with multimodal assistance. arXiv preprint arXiv:2409.11010, 2024. 2
- [18] Alec Radford, Jong Wook Kim, Chris Hallacy, Aditya Ramesh, Gabriel Goh, Sandhini Agarwal, Girish Sastry, Amanda Askell, Pamela Mishkin, Jack Clark, Gretchen Krueger, and Ilya Sutskever. Learning transferable visual models from natural language supervision. In *International* Conference on Machine Learning, 2021. 2, 3, 5, 7
- [19] Aditya Ramesh, Prafulla Dhariwal, Alex Nichol, Casey Chu, and Mark Chen. Hierarchical text-conditional image generation with clip latents. arXiv preprint arXiv:2204.06125, 1 (2):3, 2022. 3
- [20] Robin Rombach, Andreas Blattmann, Dominik Lorenz, Patrick Esser, and Björn Ommer. High-resolution image synthesis with latent diffusion models. In *Proceedings of* the IEEE/CVF conference on computer vision and pattern recognition, pages 10684–10695, 2022. 2, 3, 6
- [21] Seyedmorteza Sadat, Jakob Buhmann, Derek Bradley, Otmar Hilliges, and Romann M Weber. Cads: Unleashing the diversity of diffusion models through condition-annealed sampling. arXiv preprint arXiv:2310.17347, 2023. 2, 3, 6
- [22] Chitwan Saharia, William Chan, Huiwen Chang, Chris Lee, Jonathan Ho, Tim Salimans, David Fleet, and Mohammad Norouzi. Palette: Image-to-image diffusion models. In *ACM SIGGRAPH 2022 conference proceedings*, pages 1–10, 2022. 2
- [23] Axel Sauer, Dominik Lorenz, Andreas Blattmann, and Robin Rombach. Adversarial diffusion distillation. In *European Conference on Computer Vision*, pages 87–103. Springer, 2024. 3
- [24] Jiaming Song, Chenlin Meng, and Stefano Ermon. Denoising diffusion implicit models. *arXiv preprint arXiv:2010.02502*, 2020. 2, 3, 6
- [25] Bailey Trang, Parham Saremi, Alan Q Wang, Fangrui Huang, Zahra TehraniNasab, Amar Kumar, Tal Arbel, Li Fei-Fei, and Ehsan Adeli. Discovering latent graphs with gflownets for diverse conditional image generation. arXiv preprint arXiv:2510.22107, 2025. 3
- [26] Lvmin Zhang, Anyi Rao, and Maneesh Agrawala. Adding conditional control to text-to-image diffusion models. In *Proceedings of the IEEE/CVF International Conference on Computer Vision*, pages 3836–3847, 2023. 2
- [27] Guangcong Zheng, Xianpan Zhou, Xuewei Li, Zhongang Qi, Ying Shan, and Xi Li. Layoutdiffusion: Controllable diffusion model for layout-to-image generation. In *Proceedings* of the IEEE/CVF Conference on Computer Vision and Pattern Recognition, pages 22490–22499, 2023. 2